# 8. Influence of Uplift, Weathering, and Base Cation Supply on Past and Future CO_2 Levels

Jacob R. Waldbauer and C. Page Chamberlain

8.1 Tectonics, Rock Weathering, and CO_2 Drawdown

The weathering of silicate minerals has long been recognized as one of the dominant controls on atmospheric CO_2. A pair of well-known reactions (Urey 1952) summarizes a series of biogeochemical processes that begin with the weathering of calcium and magnesium silicates and end with the burial of Ca-Mg carbonates in marine sediments:

$$CO_2 + CaSiO_3 \leftrightarrow CaCO_3 + SiO_2$$
$$CO_2 + MgSiO_3 \leftrightarrow MgCO_3 + SiO_2$$
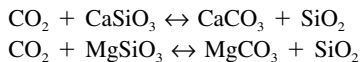
The net result is that, for each mole of calcium or magnesium silicate weathered on the continents, one mole of carbon dioxide is sequestered in marine carbonate. Thermal decomposition of these carbonates releases the CO_2 back into the atmosphere. Along with fixation of CO_2 by plants and its release during oxidative weathering of organic matter, silicate weathering is the major process controlling atmospheric CO_2 levels on the multimillion-year timescale (Berner and Kothavala 2001).

In addition to causing this direct effect on atmospheric CO_2, rock weathering can influence carbon dioxide levels indirectly. In many ecosystems, the weathering of rock containing elements essential for plant growth (including Ca, Mg, K, and P) is a primary source of these nutrients. A deficit of cation nutrients

can inhibit plant communities' capacity as CO_2 sinks by acting as the limiting factor in the synthesis of new biomass. Recently, increasing attention has been paid to declining levels of cation nutrients in forest ecosystems, particularly in the eastern United States (Federer et al. 1989; Bailey et al. 1996; Huntington et al. 2000). The prospect of large forests serving as long-term sinks for anthropogenic CO_2 is contingent upon the continued availability of base cations, a nutrient pool vulnerable to depletion by acid rain (Likens, Driscoll, and Buso 1996). In order to realistically gauge the potential for further forest growth, then, quantification of weathering rates and consequent base cation supplies is essential.

In discussions of rock weathering, there is an important distinction to be drawn between physical and chemical mechanisms. Broadly, physical weathering produces solids that are transported without significant chemical alteration as small water- or windborne particles. Chemical weathering, by contrast, releases dissolved solutes, the products of chemical alteration of primary minerals. The two types of processes reinforce each other. Chemical weathering disaggregates solid rock, increasing susceptibility to physical removal, while physical weathering fractures rock and increases the amount of mineral surface area accessible to water (White and Brantley 1995). Chemical weathering and physical weathering are quite distinct, however, in their effects on biological and atmospheric systems. Only chemical weathering draws down carbon dioxide from the atmosphere, and only chemical weathering directly produces soil nutrients, such as calcium, magnesium, and potassium, that are usable by plants.

A large number of variables exert influence on rates of rock weathering. Mineralogy of the bedrock is of primary importance, as the types of minerals present and their cation content will determine both how much CO_2 will be consumed by their weathering as well as how much nutrition the rock might supply to plants growing on its surface. The effect of climate on weathering rates has received significant attention, not least because weathering, in its role as a CO_2 sink, has a reciprocal effect on climate. White and Blum (1995) found a significant increase in weathering rates in granitic catchments with both temperature and precipitation, a trend that has been incorporated into global CO_2 models (Berner 1995). A persistent difficulty in quantifying the effects of climate on weathering has been isolating individual climatic variables from each other and from such factors as geomorphology, tectonics, vegetation, and lithology, a problem exacerbated by increasing the scale of investigation (White et al. 1999b).

The other major factor in determining long-term, large-scale weathering rates is tectonic uplift. Ultimately, it is uplift that exposes fresh continental material to weathering and so determines the total amount of weatherable material on Earth's surface. A problem in incorporating the role of uplift and mountain building into global CO_2 models is the lack of a clear paleoindicator of continental weathering rates. The strontium isotope composition of ocean water has been used as such a proxy (Raymo and Ruddiman 1992; Richter, Rowley, and DePaolo 1992), but the interpretation of the seawater Sr record is not so straight-

forward (Blum 1997; Berner and Kothavala 2001). The role of uplift in setting weathering rates, though incompletely quantified, is nevertheless essential to the global carbon cycle, as shown by the strong correlation of chemical and physical weathering rates in many world rivers (Gaillardet et al. 1999). Riebe et al. (2001) found that, for a group of granitic catchments in the Sierra Nevada Mountains, tectonics rather than climate is the decisive factor controlling long-term weathering rates.

In this paper, we present an analytical model for steady-state chemical weathering with an emphasis on the effect of uplift on the total rate of weathering in a depth profile. The model is parameterized in terms of the effective surface age, which allows comparisons of widely disparate tectonic regimes. From this model, we derive supply rates of base cation nutrients (Ca, Mg, and K) and discuss the implications for long-term CO_2 sequestration by forests. We also model the effect of the presence of disseminated hydrothermal calcite on the Sr isotope composition of weathered material and discuss how this affects interpretation of the seawater strontium record.

8.2 Modeling Steady-State Chemical Weathering

We sought to develop a model for steady-state chemical weathering for the case where uplift provides a constant supply of fresh rock to the bottom of the weathering zone and physical erosion removes incompletely weathered material from the surface at an equivalent rate. These conditions produce an unchanging total soil depth and stable flux of cations from the chemical weathering of parent rock. The situation is diagrammed in Fig. 8.1. Of particular interest is how variations in uplift velocity (and hence in supply rate of fresh material) affect the flux of cations from the weathering profile.

This balance of erosion and uplift occurs most clearly in active tectonic environments known as steady-state orogens (Koons 1990; Willet, Slingerland, and Hovius 2001). At convergent plate boundaries, thickening of the crust leads to high uplift rates due to isostasy. The rise of mountain belts results in an increase in erosion rates due to the additional relief (Ahnert 1970) and increased precipitation (Willet 1999). These two competing processes, uplift and erosion, reach a dynamic balance and create stable large-scale topography. Under these conditions, rock moves through into the weathering zone at relatively high velocities (on the order of millimeters per year), is partially chemically altered in the weathering zone, and is physically removed at the surface quickly enough to maintain a constant weathering profile. These steady-state orogens are found in essentially all active tectonic areas.

Beginning with unweathered rock of known composition, we modeled the chemical weathering rate of the various constituent minerals and the total release of cations from the weathering profile as material moves from the bottom of the weathering zone to the surface at constant velocity. Under semi-neutral conditions (pH ~5–8), chemical weathering rate is independent of pH and the kinetics of dissolution are zeroth order with respect to water (Sverdrup 1990).
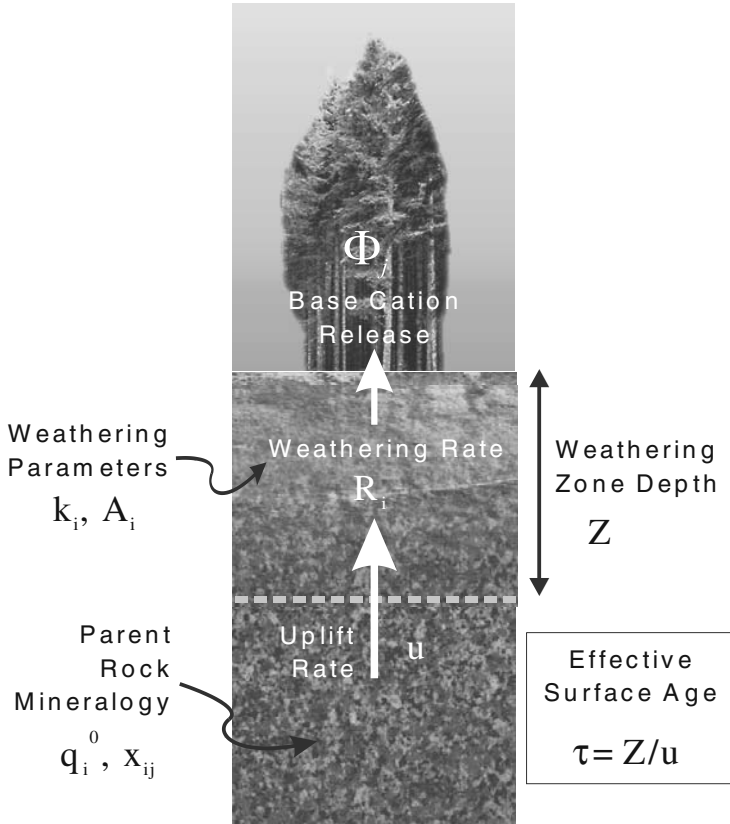
Figure 8.1. Diagram of steady-state chemical weathering model parameters and processes. Rock containing an initial (unweathered) concentration q_i^0 of mineral i is pushed upward with uplift velocity u into the weathering zone, which extends to a depth Z below the surface. In the weathering zone, the mineral weathers at a rate (R_i) dependent on the dissolution rate (k_i) and the mineral specific surface area (A_i). The model is parameterized in terms of the effective surface age, $\tau = Z/u$. Cation release rates (Φ_j) are calculated from mineral weathering rates and cation stoichiometry of the parent rock minerals (x_{ij}).

The change in concentration q_i (in mol/m³) of a mineral i with time due to chemical weathering can be expressed as a function of the dissolution rate k_i (in units of mol/m²/s) and the mineral specific surface area A_i (in m²/mol):

$$\frac{dq_i}{dt} = -k_i A_i q_i \tag{8.1}$$

In the steady state described by this model, the weathering profile remains constant; that is, the composition of material as a function of depth within the weathering zone does not change with time. Hence the condition that $(\partial q_i\, \partial t)_z = 0$, and we may write:

$$\left(\frac{\partial q_i}{\partial t}\right)_z = 0 = -k_i A_i q_i - \frac{dz}{dt}\left(\frac{\partial q_i}{\partial z}\right)_t \tag{8.2}$$

In a state of steady uplift at a velocity u, $z = ut$ where $z = t = 0$ at the bottom of the weathering zone.

Thus $dz/dt = u$, and the solution of Equation 8.2 for the concentration as a function of distance from the bottom of the weathering zone is:

$$q_i(z) = q_i^0 \exp\left[-k_i A_i \frac{z}{u}\right] \tag{8.3}$$

where q_t^0 is the concentration of the mineral in the unweathered rock. Equation 8.3 describes how the concentration of a particular mineral changes as the host rock moves through the weathering zone. Of interest, however, is the total rate of chemical weathering in the entire weathering profile. This rate can be calculated by integrating this changing concentration over the depth of the weathering profile Z:

$$R_i' = -\frac{dq_i}{dt} = k_i A_i \int_0^z q_i(z)dz = q_i^0 u\left[1 - \exp\left(-k_i A_i \frac{Z}{u}\right)\right] \tag{8.4}$$

Equation 8.3 gives the rate at which mineral i weathers as a function of weathering zone depth Z and uplift rate u. Note that R_i' is in units of mol/(m²·s): i.e., it is a rate normalized to (ground) surface area. We can define an effective surface age τ, which is the amount of time it takes for rock to move from the lower boundary of the weathering profile to the surface, as

$$\tau = \frac{Z}{u} \tag{8.5}$$

The notion of effective surface age is a useful one, as it allows the weathering rate to be expressed as a function of a single variable. This can be done by normalizing the weathering rate instead to *volume* of weathering profile; we define $R_i = R_i'/Z$ so that the weathering rate R_i is now in units of mol/(m³·s) and express the weathering rate of mineral i in terms of the effective surface age τ as:

$$R_i = \frac{q_i^0}{\tau}\left[1 - \exp(-k_i A_i \tau)\right] \tag{8.6}$$

Assuming complete and rapid physical weathering upon reaching the surface, the effective surface age is the timescale for chemical weathering of parent rock. The parameters that determine τ, the weathering zone depth Z (also termed the depth to bedrock), and the uplift velocity u are variables that are directly observable in the field. Furthermore, Z and u are regional quantities, whose values are generally uniform over relatively large areas of Earth's surface. This relationship makes the effective surface age a useful metric for comparing weathering rates in different tectonic regimes on a global scale.

It should be emphasized that effective surface ages vary greatly in differing tectonic environments. In an active collisional orogen like the Himalayas or Andes, uplift rates can be as high as 10 mm/yr and weathering zones are about 2 m deep, resulting in an effective surface age of 200 years. By contrast, a tectonically inactive craton in a tropical climate can be uplifting at only .01 mm/yr or less, while the weathering zone might be 30 m or deeper, so effective surface ages in these environments are in the range of 3–10 million years. This five-orders-of-magnitude range in effective surface ages is attributable more to the range of uplift rates across the globe (~four orders of magnitude) than to variations in the depth-to-bedrock (~two orders of magnitude); hence, effective surface age is more (though not exclusively) a measure of tectonic uplift than of weathering profile depth. It should also be recognized that uplift rate and weathering zone depth are not entirely independent, as very deep weathering profiles simply do not develop on rapidly uplifting bedrock, nor do stable cratons persist with only thin veneers of soils on top.

In order to recover quantitative estimates of chemical weathering rates from Equation 8.6, values of the specific surface area (A_i) for all the minerals of interest are required. Establishing accurate and consistent values for the specific surface area of minerals has been a difficult problem (see, e.g., Hochella and Banfield 1995; Brantley, White, and Hodson 1999; Gautier, Oelkers, and Schott 2001), and field and laboratory measurements are often at odds. For this model we chose to take the specific surface area to be the product of the geometric surface area for a given particle size and the surface roughness SR_i, defined as the ratio of the experimental BET surface area (measured by gas-adsorption methods) to the calculated geometric surface area (Sverdrup 1990; White 1995). This method, while perhaps an imprecise estimate of the true reactive surface area of a mineral grain, is the most direct method to obtain a self-consistent set of surface area values over a range of grain sizes and mineral types. Taking this approach, the weathering rate is:

$$R_i = \frac{q_i^0}{\tau} \left[1 - \exp\left(-\frac{6k_i SR_i}{\rho_i d_i} \tau \right) \right] \tag{8.7}$$

where ρ_i is the molar density of the mineral, d_i is the grain size (diameter of an assumed spherical grain), and SR_i is the surface roughness.

Estimates of the flux of base cation nutrients from a weathering profile can be made from this formula if the rock composition is known in detail. If a mole of mineral i contains x_{ij} moles of cation species j (e.g., for anorthite, $CaAl_2Si_2O_8$, $x_{An,Ca}=1$), then the flux, Φ_j, of that cation per cubic meter of weathering profile is:

$$\Phi_j = \sum_8 x_{ij} R_i \tag{8.8}$$

A value for the total flux from a catchment is obtained by multiplying the cation flux Φ_j by the volume of weathering profile in the catchment (its surface area times the depth of the weathering profile Z).

This model is admittedly simplified in several points. First, we assume that the weathering profile is in a steady state and does not change significantly in depth. This assumption certainly holds in the steady-state orogen described above and may be essentially valid for a broader range of circumstances (Heimsath et al. 1997). However, areas undergoing rapid physical erosion uncompensated by uplift, or where the soil profile is thickening significantly, will clearly fall outside its scope. Therefore, this model applies best to weathering-limited conditions (Stallard and Edmond 1983) where transport of weathered material is unhindered.

Second, we ignore the production of secondary minerals, such as clays, during the weathering of silicates. Since clay minerals contain very small amounts of the base cations of primary interest here, this step can be justified. However, the release of elements that are major constituents of clays, such as aluminum, cannot be calculated in the way described above, as they will be strongly retained in the soil profile. The availability of phosphorus, too, cannot be accurately predicted because of the complexation of phosphate with iron in secondary minerals. As shown by Walker and Syers (1976) in their study of New Zealand soils, weathering of apatite initially releases phosphate, but as the soil profile develops, more and more phosphate is complexed with Fe and becomes unavailable to plants. A third simplifying assumption is that all minerals begin weathering at the same depth and mineral surface reactivity remains essentially constant, which may not hold true in some environments (White et al. 2001). The effects of these assumptions do not, we feel, outweigh the overriding fact that uplift determines the rate at which fresh bedrock is exposed to weathering, and thereby tectonics plays a decisive role in weathering on a global scale.

8.3 Model Results: Comparison of CO_2 Drawdown and Base Cation Supply Between Tectonic Regimes

In Fig. 8.2 and Fig. 8.3, we show the results of this steady-state weathering model for the weathering of a rock of typical granitic composition, 20% quartz (SiO_2; $k_i = 1 \times 10^{-15}$), 25% orthoclase feldspar ($KAlSi_3O_8$; $k_i = 4 \times 10^{-13}$), 40% oligoclase feldspar ($Ca_2Na_8Al_{1.2}Si_{2.8}O_8$; $k_i = 3 \times 10^{-12}$), and 15% biotite ($KMg_{1.2}Fe_{1.8}(AlSi_3O_{10})(OH)_2$; $k_i = 6 \times 10^{-13}$). Indicated on the figures are ranges of effective surface ages characteristic of different tectonic environments.

The chemical weathering rate of the granitic substrate declines sharply with increasing surface age (Fig. 8.2A), dropping by more than an order of magnitude between typical active orogen effective surface ages and temperate craton conditions. For areas with $\tau > 100,000$ yr, the chemical weathering rate is very low, and for the oldest (i.e., slowest-uplifting, thickest-mantled) tropical cratons, the rate is approx 10^{-11} mol/($m^3 \cdot s$). These results are in general agreement with published measurements of weathering rates, as shown in Fig. 8.2B), which plots the observed annual silicon discharge from a range of world rivers against ef-
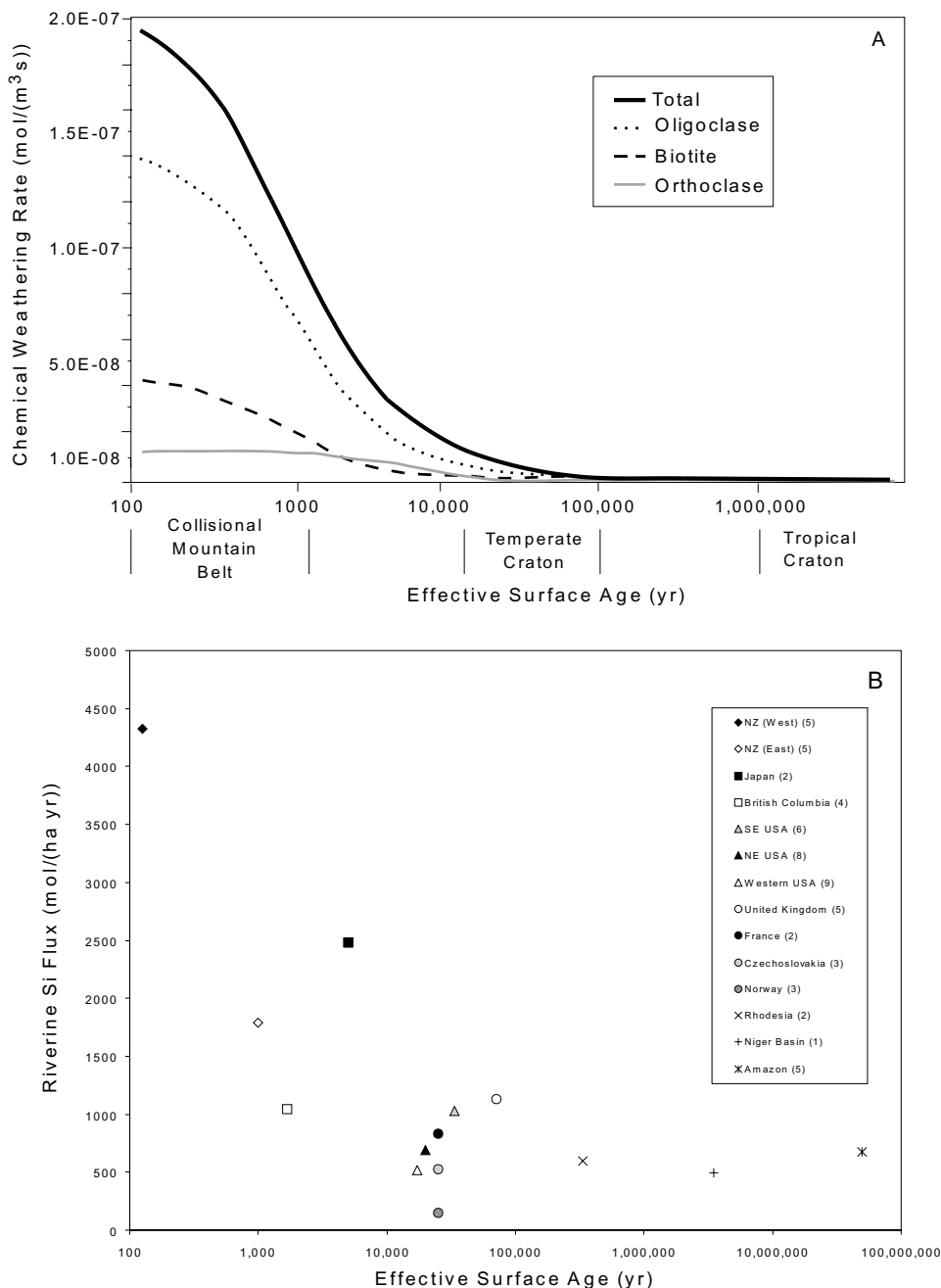
Figure 8.2. **(A)** Results of steady-state chemical weathering model for granitic material. Ranges of effective surface age values for different tectonic regimes are indicated. **(B)** Riverine silicon fluxes as a function of effective surface age for a number of world rivers. Numbers following labels in legend indicate number of measurements averaged to give the value for a particular area. Data from: Schaer et al. (1975); Kronberg et al. (1979); Miller and Lakatos (1983); Bierman et al. (1993); Tippet and Kamp (1993); Kelsey and Bockheim (1994); Simpson et al. (1994); White and Blum (1995); Gaillardet et al. (1997); Glasser and Hall (1997); Small et al. (1997); Boeglin and Probst (1998); Viers et al. (2000); Hiroshi et al. (2001); Jacobson et al. (2003).

fective surface age for the area in question. Riverine silicon is a useful field index for rock weathering because it derives almost entirely from the weathering of silicate minerals and its flux is not skewed by the presence of trace amounts of carbonates, oxides, or sulfides in the parent rock.

In Fig. 8.3 we show a similar comparison for release rates of base cations (Ca, Mg, and K). The cation release rate is very high in active orogen conditions and drops to negligible amounts on landscapes with $\tau > 100,000$ yr. As seen in Fig. 8.3B (note logarithmic scale), the observed cation fluxes do not decrease substantially for areas with greater surface ages. This is likely because of the lower bound on total flux due to atmospheric deposition, an input not taken into account in our model. The implication is that plant communities growing on high effective surface age landscapes are dependent primarily on atmospheric deposition to supply them with base cation nutrients, a suggestion supported by studies of forests growing on tropical cratons (Salati and Vose 1984; Markewitz et al. 2001).

The markedly higher weathering rates of low effective surface age environments mean that weathering in tectonically active areas is expected to draw down significantly more CO_2 than weathering in tectonically inactive areas. Hence, it is in the building of large mountain belts that the greatest amount of atmospheric carbon dioxide can be sequestered in marine carbonate. This result of the steady-state chemical weathering model is in good accord with the recent detailed field study of Mortatti and Probst (2003), who found that the Andes region accounts for 78% of CO_2 drawdown by silicate weathering in the Amazon basin. The largest orogens, for example the Himalayas, are likely to be recorded in the geochemical record; the interpretation of the strontium isotope composition of marine carbonates in this regard is discussed in the next section.

It should be remembered that this model calculates weathering rates normalized to volume of weathering profile. As a result, accurate comparison of large-scale weathering rates between environments depends on quantification of both exposed surface area and the depth at which weathering begins. In principle, one can use a model of this type—suitably extended to a variety of parent rock lithologies—to predict which areas of Earth's surface are the most active sinks for atmospheric CO_2. The importance of a large, tectonically active area such as the Himalayan chain is clear. Calculating the relative impact of weathering of a smaller orogen, such as the Southern Alps of New Zealand, is far more complicated. To obtain useful estimates of weathering in the disparate environments of these relatively small regions, a model would have to incorporate the nontrivial effects of climate (both temperature and precipitation), vegetation, and microbial activity, as well as factor in the geographical preponderance of weathering-limited versus transport-limited erosion regimes. For many of these variables, the requisite data simply do not exist on a global scale. As such, a comprehensive model of rock weathering and its effect on atmospheric CO_2 is still some ways off. It is clear from this model, though, that any attempt to calculate long-term, large-scale weathering rates must incorporate the effects of tectonic uplift.
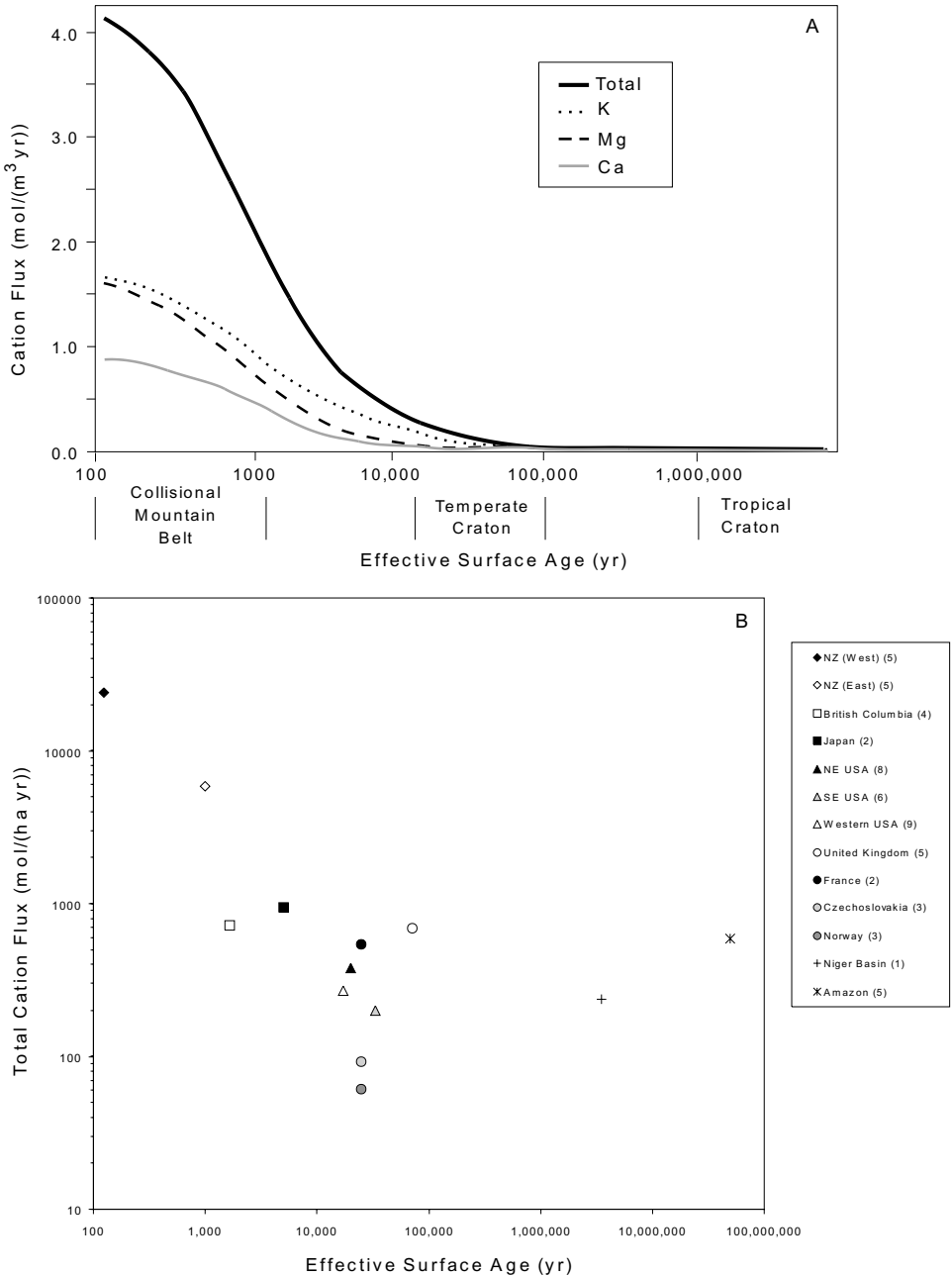
A

Cation Flux (mol/(m³ yr))

4.0

3.0

2.0

1.0

0.0

— Total
··· K
– – Mg
— Ca

100   1000   10,000   100,000   1,000,000

Collisional Mountain Belt

Temperate Craton

Tropical Craton

Effective Surface Age (yr)

B

Total Cation Flux (mol/(ha yr))

100000

10000

1000

100

10

100   1,000   10,000   100,000   1,000,000   10,000,000   100,000,000

Effective Surface Age (yr)

◆ NZ (West) (5)
◇ NZ (East) (5)
□ British Columbia (4)
■ Japan (2)
▲ NE USA (8)
△ SE USA (6)
△ Western USA (9)
○ United Kingdom (5)
● France (2)
◉ Czechoslovakia (3)
◐ Norway (3)
+ Niger Basin (1)
✗ Amazon (5)

Figure 8.3. (A) Results of steady-state chemical weathering model for cation release from granitic material. Ranges of effective surface age values for different tectonic regimes are indicated. (B) Riverine cation fluxes as a function of effective surface age for a number of world rivers (note logarithmic scale). Numbers following labels in legend indicate number of measurements averaged to give the value for a particular area. Data from sources as in Fig. 8.2.

8.4 Interpretation of the Marine Strontium Isotope Record and Past CO$_2$ Drawdown

In order to reconstruct the history of atmospheric CO$_2$, it is necessary to have some information about the past continental rock weathering rates, as the weathering of silicate minerals serves as a major sink for atmospheric CO$_2$. One proxy that has been used to estimate past continental rock weathering is the strontium isotope composition of marine carbonates. The mechanism for the proxy is as follows: continental weathering of calcium silicates, rich in [87]Sr from the decay of [87]Rb, draws down CO$_2$ and produces dissolved carbonate (with a high [87]Sr/[86]Sr ratio) in the oceans. This carbonate precipitates out of seawater to form carbonate minerals in marine sediments. An observed increase [87]Sr/[86]Sr ratio of these marine carbonates, then, can be interpreted as an increase in continental weathering rates. The past 40 million years have seen a marked increase in the seawater [87]Sr/[86]Sr ratio, a trend attributed to the India-Asia collision and consequent uplift of the Himalayas, which exposed large amounts of fresh granitic rock to weathering and possibly sequestered large amounts of atmospheric CO$_2$ in marine sediments (Edmond 1992; Richter, Rowley, and DePaolo 1992).

The strontium isotope composition of rock at Earth's surface is set by two factors: first, by the [87]Sr/[86]Sr ratio of the constituent minerals at their closure temperature for strontium, which is typically about 300°C and achieved at about 15 km depth. At this point, strontium exchange between each mineral and any surrounding fluids stops. Second, the [87]Sr/[86]Sr ratio of a mineral can increase due to the decay of [87]Rb to [87]Sr with a half-life of 48.8 Gyr. Uplift is critical for this second factor, because it determines how long it takes for a mineral to be brought from the closure depth to the surface where it can be weathered. Hence uplift will determine how much time [87]Rb has to decay and therefore the ultimate [87]Sr/[86]Sr ratio of the weathered material. Taking a closure depth of 15 km and using the decay constant for [87]Rb, $\lambda = 1.42 \times 10^{-11}$ yr^{-1} (Steiger and Jäger 1978), the [87]Sr/[86]Sr ratio of rock at the earth's surface can be written

$$(^{87}Sr/^{86}Sr)_{surface} = (^{87}Sr/^{86}Sr)_0 + (^{87}Rb/^{86}Sr)_0 (e^{\lambda(15km/u)} - 1) \qquad (8.9)$$

where the subscript 0 indicates the isotopic ratios at the closure temperature and u is the uplift velocity in km/yr. With knowledge of the initial [87]Sr and [87]Rb content of the rock, this equation provides a value for the strontium isotope composition of material weathering at the surface, which is the first step towards modeling how tectonics can influence the seawater Sr record.

A complication in the interpretation of the seawater strontium isotope record is the presence in many active orogen systems (including the Himalayas) of disseminated hydrothermal calcite. Large hydrothermal systems are a common feature of active collisional mountain belts (Koons and Craw 1991; Chamberlain

et al. 1995). These hydrothermal systems are most vigorous in the areas of high uplift rates that have steep topography and an elevated brittle/ductile transition. A common feature of these hydrothermal systems is the abundant, secondary disseminated calcite within silicate rocks (Gazis et al. 1998; Templeton et al. 1998; White et al. 1999a). Recent work has shown that this calcite has elevated $^{87}Sr/^{86}Sr$ ratios as a result of equilibration with primary silicate minerals (Blum et al. 1998). Because calcite weathers far more rapidly than the host silicate minerals, the $^{87}Sr/^{86}Sr$ ratios of water in streams in these areas of rapid uplift are in large part dominated by weathering of calcite. It is, therefore, difficult if not impossible to distinguish calcite from silicate weathering with $^{87}Sr/^{86}Sr$ ratios alone.

Inclusion of even a small amount of interstitial calcite has a strong effect on the strontium flux from granitic rock due to weathering. This effect is shown in Fig. 8.4, Panel A, where 3% calcite ($CaCO_3$; $k_i = 1 \times 10^{-5}$) has been added to the granite composition described in the previous section, and $^{87}Rb/^{86}Sr$ ratios measured by Gazis et al. (1998) for a typical Himalayan granite included for the constituent minerals (oligoclase, .05; biotite, 441.4; orthoclase, 1.01). Representative strontium concentrations for minerals were obtained from Gazis et al. (1998) for oligoclase (128.2 ppm), biotite (3.5 ppm), and orthoclase (312.2 ppm) and from Jacobson and Blum (2000) for calcite (622.7 ppm). The calculated contribution of calcite to the total amount of strontium weathered from the rock is as high as 35% in tectonically active conditions, reflecting calcite's high Sr content and rapid weathering.

The calculated effect of the disseminated calcite on the isotopic composition of the weathered strontium is evident in Fig. 8.4B. The secondary, disseminated calcite dominates the strontium flux from low effective surface age areas, holding the $^{87}Sr/^{86}Sr$ ratio essentially constant over a range of tectonic conditions from active orogens to temperate cratons. As shown in the previous section, there is a tenfold decrease in the total chemical weathering rate over the same range. This result indicates that, where disseminated calcite is present, the isotopic composition of weathered Sr is insensitive to large changes in chemical weathering rate. Disseminated hydrothermal calcite has its largest effects on the Sr content of weathered material in tectonically active areas, which are precisely the places where weathering rates are highest and the most CO_2 is being drawn down. Furthermore, this model predicts that the most radiogenic strontium derives from regions of low total Sr flux, areas where silicate weathering consumes little atmospheric CO_2. Such a trend was reported by Lear et al. (2003) in their study of the Cenozoic benthic foraminiferal Sr/Ca record and reconstruction of global riverine Sr flux and isotopic composition. These results complicate interpretation of the seawater Sr isotope record, as they suggest that the isotopic composition of weathered strontium is not a clear index of the rate of continental silicate weathering.
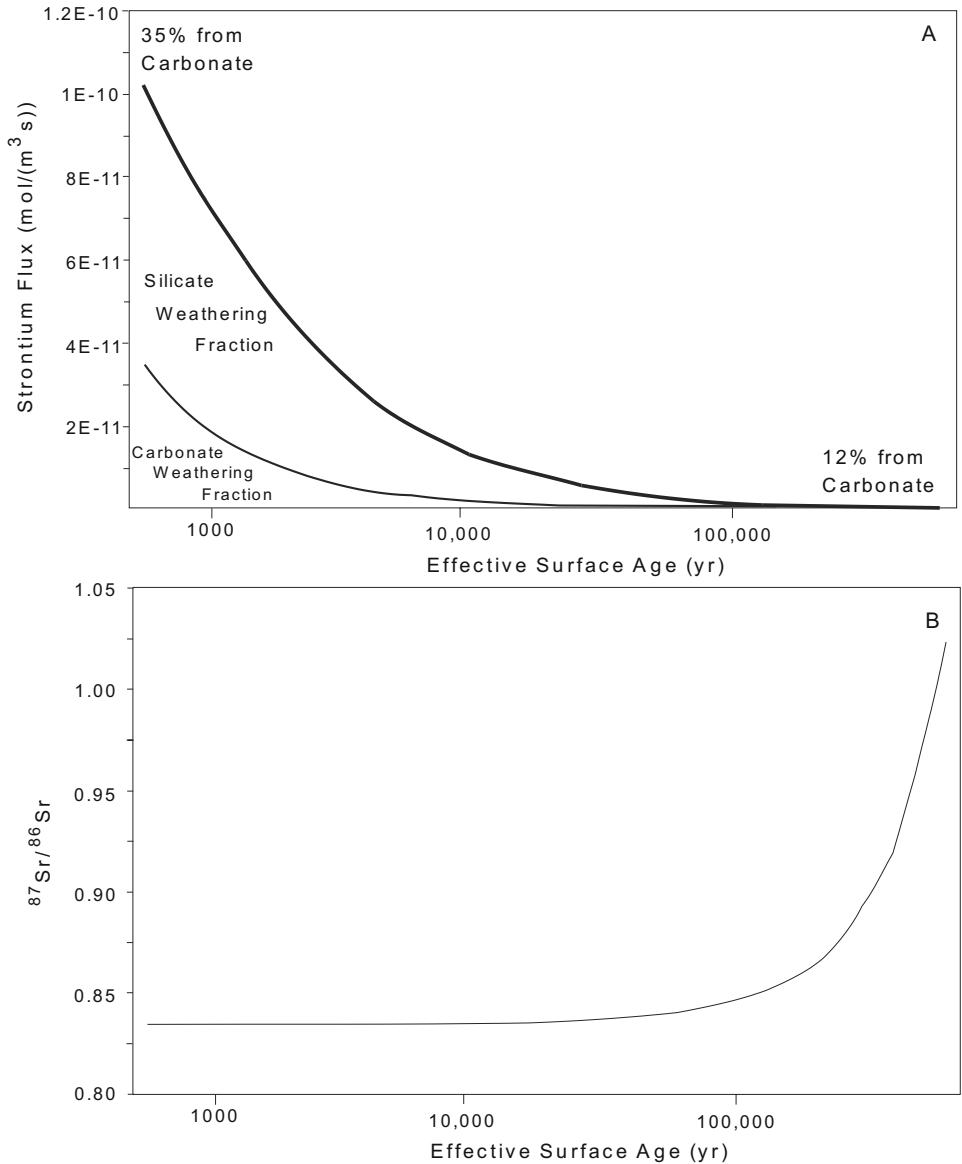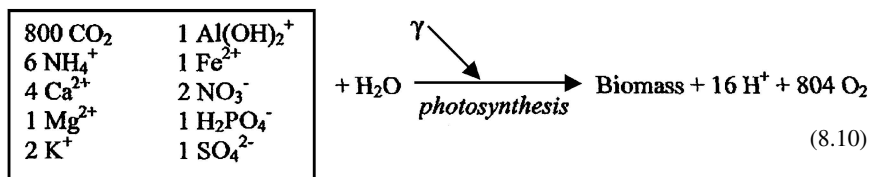
Figure 8.4. (A) Calculated Sr flux from weathering of granite with 3% disseminated calcite. The contribution of carbonate weathering to the total Sr flux ranges from 12% at $\tau = 650,000$ yr to 35% at $\tau = 500$ yr. **(B)** Calculated $^{87}Sr/^{86}Sr$ ratio of weathered material. The weathering of 3% calcite holds the isotopic composition essentially constant over a large range of effective surface ages; the total chemical weathering rate drops significantly over the same range. The most radiogenic Sr comes from regions with low total Sr flux.

8.5 Implications of Forest Base Cation Supply for Long-Term Sequestration of CO_2

The weathering of minerals containing base cations useful to plants (including Ca, K and Mg) is an important source of nutrients for many ecosystems (Waring and Schlesinger 1985). The stoichiometry for the growth of plant biomass by photosynthesis is approximately (Schnoor and Stumm 1985; Drever and Clow 1995):

$$\begin{array}{ll} 800\ CO_2 & 1\ Al(OH)_2^+ \\ 6\ NH_4^+ & 1\ Fe^{2+} \\ 4\ Ca^{2+} & 2\ NO_3^- \\ 1\ Mg^{2+} & 1\ H_2PO_4^- \\ 2\ K^+ & 1\ SO_4^{2-} \end{array} \quad +\ H_2O \quad \xrightarrow[\text{photosynthesis}]{\gamma} \quad \text{Biomass} + 16\ H^+ + 804\ O_2$$

$$(8.10)$$

At present atmospheric CO_2 levels, carbon dioxide is often a limiting nutrient for the synthesis of biomass in C_3 plants. Throughout the Phanerozoic, however, atmospheric CO_2 has repeatedly reached concentrations 10 or more times present levels (Berner and Kothavala 2001). At such high concentrations, CO_2 would cease to be a limiting nutrient and the supply of other species, principally nitrogen and the base cations, would determine plant growth rates. As anthropogenic inputs increase modern atmospheric CO_2 levels, there is the potential that an increase in total plant biomass—the greening of Earth's forests—might serve as a long-term sink for human-produced carbon dioxide. Such a sink will only be sustainable so long as the other requisite nutrients for plant growth are readily available and do not limit photosynthesis. Clearly, an understanding of how weathering supplies these nutrients to ecosystems is a prerequisite for both reconstructing how plants have responded to past changes in CO_2 levels and predicting how much carbon dioxide might be sequestered in present-day forests.

A growing body of evidence suggests that forest ecosystems may become cation-limited (and especially calcium-limited), particularly as a result of watershed acidification. Studies pointing to this conclusion have been carried out in both the northeastern (Federer et al. 1989; Bailey et al. 1996; Lawrence et al. 1997, 1999; Yanai et al. 1999) and southeastern United States (DeWalle et al. 1999; Huntington et al. 2000; Huntington 2000), as well as at several sites in Europe (Kram et al. 1997; Fichter et al. 1998). All of these areas would fall on the plots in Fig. 8.3 under the grouping of temperate cratons: i.e., areas with relatively low rates of base cation release due to weathering. Interestingly, human activity appears to have also significantly reduced atmospheric base cation deposition in these regions (Hedin et al. 1994).

As shown above, our model predicts much greater fluxes of base cations due to weathering under low effective surface age conditions. The implication is that base cations will not become limiting nutrients for forests growing in tectoni-

cally active areas. It is forests in these regions that are best suited to serve as long-term sinks for anthropogenic CO_2. These forests are also the least susceptible to soil nutrient leaching due to watershed acidification, since they receive a steady supply of nutrients from the weathering of fresh bedrock. Areas such as the eastern United States, on the other hand, are more vulnerable to losses due to acid rain, especially because a greater proportion of their forests' cation supplies comes from atmospheric deposition.

8.6 Summary

Tectonic uplift, through its control of chemical weathering rates—and, therefore, control of base cation supply rates to forests—exerts a powerful influence on atmospheric carbon dioxide. The analytical model presented in this paper quantifies the role of uplift in setting bulk weathering rates and demonstrates that areas with low effective surface ages (i.e., tectonically active areas) are likely to play the largest role as land-based CO_2 sinks. This is important both for reconstructing the history of atmospheric CO_2 and for predicting how and where human activity might have the most profound impacts on the global carbon dioxide cycle.

An interesting consideration in the discussion of the relationship between tectonics and weathering is the question of what it means for a landscape to be in a steady state. Over the longest periods, changes in plate motions will ultimately determine the condition of a particular tectonic environment, but shorter-timescale processes, especially glaciation, are also important. This question becomes particularly relevant to studies of atmospheric carbon dioxide because many of the northern latitude forest regions to which a great deal of CO_2 drawdown has been attributed have recently been glaciated. The forested temperate cratons, with effective surface ages in the 100,000-year range, sit on the border between weathering-dominated and atmosphere-dominated cation nutrient supplies.

Blum (1997) found that glacial soils in the Wind River Mountains younger than about 138,000 years had chemical weathering accelerated over steady-state rates. This span is close to the effective surface age, the amount of time the model presented here would predict it would take for material to move through the weathering profile in that environment. The implication is that forests growing on this terrain since the last glaciation have been supported by nutrient supplied from fresh rock exposed by the last glacial retreat, a supply that has essentially run out. If these northern latitude regions have in fact relatively recently reached a steady state with respect to weathering, they may actually become more cation limited in the future. It is worth noting that some northern areas, including parts of Canada and central Scandinavia, are still experiencing postglacial isostatic uplift. If the glacial-interglacial timescale is shorter than the time required to develop a constant weathering profile, then some areas may never actually reach what could be called a steady state.

The prospect of developing a global model for rock weathering that includes the combined effects of tectonics, climate, vegetation, and human activity along with glaciation, volcanism, and other geologic and geomorphic processes is a daunting one. The model presented here demonstrates, however, that a relatively simple framework can capture many of the main effects. Apparent areas for expansion of the scope of this model include quantifying the timescale for weathering profile development after glaciation, as well as the effects of the production and weathering of secondary minerals on release and retention of nutrients. Nevertheless, these additional factors will not mask the major role played by tectonic uplift and rock weathering in the dynamics of atmospheric CO_2 on a global scale.

References

Ahnert, F. 1970. Functional relationships between denudation, relief, and uplift in large mid-latitude drainage basins. *American Journal of Science* 268:243–63.

Bailey, S.W., J.W. Hornbeck, C.T. Driscoll, and H.E. Gaudette. 1996. Calcium inputs and transport in a base-poor forest ecosystem as interpreted by Sr isotopes. *Water Resources Research* 32:707–19.

Berner, R.A. 1995. Chemical Weathering and Its Effect on Atmospheric CO_2 and Climate. *Reviews in Mineralogy* 31:565–84.

Berner, R.A., and Z. Kothavala. 2001. GEOCARB III: A revised model of atmospheric CO_2 over Phanerozoic time. *American Journal of Science* 301:182–204.

Bierman, P.R., C.A. Massey, A.R. Gillespie, D. Elmore, and M. Caffe. 1993. Erosion rate and exposure age of granite landforms estimated with cosmogenic [36]Cl. *Geological Society of America Abstracts with Programs* 25:141.

Blum, J.D. 1997. The Effect of late Cenozoic glaciation and tectonic uplift on silicate weathering rates and the marine [87]Sr/[86]Sr record. In *Tectonic uplift and climate change,* ed. W.F. Ruddiman, 260–289. New York: Plenum Press.

Blum, J.D., C.A. Gazis, A.D. Jacobson, and C.P. Chamberlain. 1998. Carbonate versus silicate weathering in the Raikhot watershed within the High Himalayan Crystalline Series. Geology 26:411–14.

Boeglin, J.-L., and J.-L. Probst. 1998. Physical and chemical weathering rates and CO_2 consumption in a tropical lateritic environment: the upper Niger basin. *Chemical Geology* 148:137–56.

Brantley, S.L., A.F. White, and M.E. Hodson. 1999. Surface area of primary silicate minerals. In *Growth, dissolution, and pattern formation in geosystems,* ed. B. Jamtveit and P. Meakin, 291–326. Dordrecht, Netherlands: Kluwer Academic Publishers.

Chamberlain, C.P., P.K. Zeitler, D.E. Barnet, D. Winslow, S.R. Poulson, T. Leahy, and J.E. Hammer. 1995. Active hydrothermal systems during the recent uplift of Nanga Parbat, Pakistan Himalaya. *Journal of Geophysical Research* 100:439–53.

DeWalle, D.R., J.S. Tepp, B.R. Swistock, W.E. Sharpe, and P.J. Edwards. 1999. Tree-ring cation response to experimental watershed acidification in West Virginia and Maine. *Journal of Environmental Quality* 28:299–309.

Drever, J.I., and D.W. Clow. 1995. Weathering rates in catchments. *Reviews in Mineralogy* 31:463–84.

Edmond, J.M. 1992. Himalayan tectonics, weathering processes, and the strontium isotope record in marine limestones. *Science* 258:1594–97.

Federer, C.A., J.W. Hornbeck, L.M. Tritton, C.M. Martin, R.S. Pierce, and C.T. Smith. 1989. Long-term depletion of calcium and other nutrients in Eastern US forests. *Environmental Management* 13:593–601.

Fichter, J., E. Dambrine, M.P. Turpault, and J. Ranger. 1998. Base cation supply in spruce and beech ecosystems of the Strengbach catchment (Vosges mountains, NE France). *Water Air and Soil Pollution* 104:125–48.

Gaillardet, J., B. Dupre, C.J. Allegre, and P. Negrel. 1997. Chemical and physical denudation in the Amazon River Basin. *Chemical Geology* 142: 141–73.

Gaillardet, J., B. Dupre, P. Louvat, and C.J. Allegre. 1999. Global silicate weathering and CO_2 consumption deduced from the chemistry of large rivers. *Chemical Geology* 159:3–30.

Gautier, J.-M., E.H. Oelkers, and J. Schott. 2001. Are quartz dissolution rates proportional to B.E.T. surface areas? *Geochimica et Cosmochimica Acta* 65:1059–70.

Gazis, C.A., J.D. Blum, C.P. Chamberlain, and M. Poage. 1998. Isotope systematics of granites and gneisses of the Nanga Parbat massif, Pakistan Himalaya. *American Journal of Science* 298:673–98.

Glasser, N.F., and A.M. Hall. 1997. Calculating Quaternary glacial erosion rates in northeast Scotland. *Geomorphology* 20: 29–48.

Hedin, L.O., L. Granat, G.E. Likens, T.A. Buishand, J.N. Galloway, T.J. Butler, and H. Rodhe. 1994. Steep declines in atmospheric base cations in regions of Europe and North America. *Nature* 367:351–54.

Heimsath, A.M., W.E. Dietrich, K. Nishiizumi, and R.C. Finkel. 1997. The soil production function and landscape equilibrium. *Nature* 388:358–61.

Hiroshi, S., O. Jun'ichi, N. Masao, and M. Yasuo. 2001. Holocene uplift derived from relative sea-level records along the coast of western Kobe, Japan. *Quaternary Science Reviews* 20:1459–74.

Hochella, M.F. Jr., and J.F. Banfield. 1995. Chemical weathering of silicates in nature: A microscopic perspective with theoretical considerations. *Reviews in Mineralogy* 31: 353–406.

Huntington, T.G. 2000. The potential for calcium depletion in forest ecosystems of southeastern United States: Review and analysis. *Global Biogeochemical Cycles* 14:623–38.

Huntington, T.G., R.P. Hooper, C.E. Johnson, B.T. Aulenbach, R. Capellato, and A.E. Blum. 2000. Calcium depletion in a Southeastern United States forest ecosystem. *Soil Science Society of America Journal* 64:1845–58.

Jacobson, A.D., and J.D. Blum. 2000. Ca/Sr and [87]Sr/[86]Sr geochemistry of disseminated calcite in Himalayan silicate rocks from Nanga Parbat: Influence on river-water chemistry. *Geology* 28:463–66.

Jacobson, A.D., J.D. Blum, C.P. Chamberlain, D. Craw, and P.O. Koons. 2003. Climatic and tectonic controls on chemical weathering in the New Zealand Southern Alps. *Geochimica et Cosmochimica Acta* 67:29–46.

Kelsey, H.M., and J.G. Bockheim. 1994. Coastal landscape evolution as a function of eustasy and surface uplift rate, Cascadia margin, southern Oregon. *Geological Society of America Bulletin* 106:840–54.

Koons, P.O. 1990. The two-sided orogen: Collision and erosion from the sand box to the Southern Alps, New Zealand. *Geology* 18:679–82.

Koons, P.O., and D. Craw. 1991. Evolution of fluid driving forces and composition within collisional orogens. *Geophysical Research Letters* 280:935–38.

Kram, P., J. Hruska, B.S. Wenner, C.T. Driscoll, and C.E. Johnson. 1997. The biogeochemistry of basic cations in two forest catchments with contrasting lithology in the Czech Republic. *Biogeochemistry* 37:173–202.

Kronberg, B.I., W.S. Fyfe, O.H. Leonardos, and A.M. Santos. 1979. The chemistry of some Brazilian soils: Element mobility during intense weathering. *Chemical Geology* 24:211–29.

Lawrence, G.B., M.B. David, S.W. Bailey, and W.C. Shortle. 1997. Assessment of soil calcium status in red spruce forests in the northeastern United States. *Biogeochemistry* 38:19–39.

Lawrence, G.B., M.B. David, G.M. Lovett, P.S. Murdoch, D.A. Burns, J.L. Stoddard, B.P. Baldigo, J.H. Porter, and A.W. Thompson. 1999. Soil calcium status and the response of stream chemistry to changing acidic deposition rates. *Ecological Applications* 9:1059–72.

Lear, C.H., H. Elderfield, and P.A. Wilson. 2003. A Cenozoic seawater Sr/Ca record from benthic foraminiferal calcite and its application in determining global weathering fluxes. *Earth and Planetary Science Letters* 208:69–84.

Likens, G.E., C.T. Driscoll, and D.C. Buso. 1996. Long-term effects of acid rain: Response and recovery of a forest ecosystem. *Science* 272:244–46.

Markewitz, D., E.A. Davidson, R. de O. Figuelredo, R.L. Victoria, and A.V. Krusche. 2001. Control of cation concentrations in stream waters by surface soil processes in an Amazonian watershed. *Nature* 410:802–805.

Miller, D.S., and S. Lakatos. 1983. Uplift rate of Adirondack anorthosite measured by fission-track analysis of apatite. *Geology* 10:284–86.

Mortatti, J., and J.-L. Probst. 2003. Silicate rock weathering and atmospheric/soil CO_2 uptake in the Amazon basin estimated from river water geochemistry: seasonal and spatial variations. *Chemical Geology* 197:177–96.

Raymo, M.E., and W.F. Ruddiman. 1992. Tectonic forcing of late Cenozoic climate. *Nature* 359:117–22.

Richter, F.M., D.B. Rowley, and D.J. DePaolo. 1992. Sr isotope evolution of seawater: the role of tectonics. *Earth and Planetary Science Letters* 109:11–23.

Riebe, C.S., J.W. Kirchner, D.E. Granger, and R.C. Finkel. 2001. Strong tectonic and weak climatic control of long-term chemical weathering rates. *Geology* 26:511–14.

Salati, E., and P.B. Vose. 1984. Amazon basin: A system in equilibrium. *Science* 225: 129–38.

Schaer, J.P., G.M. Reimer, and G.A. Wagner. 1975. Actual and ancient uplift in the Gotthard region, Swiss Alps: A comparison between precise leveling and fission-track apatite age. *Tectonophysics* 29:293–300.

Schnoor, J.L., and W. Stumm. 1985. Acidification of aquatic and terrestrial ecosystems. In *Chemical processes in lakes,* ed. W. Stumm, 475–504. New York: Wiley.

Simpson, G.D.H., A.F. Cooper, and R.J. Norris. 1994. Late quaternary evolution of the Alpine fault zone at Paringa, South Westland, New Zealand. *New Zealand Journal of Geology and Geophysics* 37:49–58.

Small, E.E., R.S. Anderson, J.L. Repka, and R. Finkel. 1997. Erosion rates of alpine bedrock summit surfaces deduced from in situ [10]Be and [26]Al. *Earth and Planetary Science Letters* 150:413–25.

Stallard, R.F., and J.M. Edmond. 1983. Geochemistry of the Amazon 2: The influence of geology and weathering environment on the dissolved load. *Journal of Geophysical Research* 88:9688–9761.

Stallard, R.F. 1995. Relating chemical and physical erosion. *Reviews in Mineralogy* 31: 543–64.

Steiger, R.H., and E. Jäger. 1978. Subcommission on Geochronology: Convention on the use of decay constants in geochronology and cosmochronology. *Studies in Geology* 6:67–71.

Sverdrup, H.U. 1990. *The kinetics of base cation release due to chemical weathering.* Lund, Sweden: Lund University Press.

Templeton, A.S., C.P. Chamberlain, P.O. Koons, and D. Craw. 1998. Stable isotopic evidence for mixing between metamorphic and surface-derived waters during uplift of the Southern Alps, New Zealand. *Earth and Planetary Science Letters* 154: 73–92.

Tippet, J.M., and P.J.J. Kamp. 1993. Fission track analysis of the late Cenozoic vertical

kinematics of continental Pacific crust, South Island, New Zealand. *Journal of Geophysical Research* 98:16,119–48.

Urey, H.C. 1952. *The planets: Their origin and development.* New Haven: Yale University Press.

Viers, J., B. Dupre, J. Braun, S. Debert, B. Angeletti, J.N. Ngoupayou, and A. Michard. 2000. Major and trace element abundances, and strontium isotopes in the Nyong basin rivers (Cameroon): Constraints on chemical weathering processes and element transport mechanisms in humid tropical environments. *Chemical Geology* 169:211–41.

Walker, T.W., and J.K. Syers. 1976. The fate of phosphorus during pedogenesis. *Geoderma* 15:1–19.

Waring, R.H., and W.H. Schlesinger. 1985. *Forest ecosystems: Concepts and management.* San Diego: Academic Press.

White, A.F. 1995. Chemical weathering rates of silicate minerals in soils. *Reviews in Mineralogy* 31:407–61.

White, A.F., and A.E. Blum. 1995. Effects of climate on chemical weathering rates in watersheds. *Geochimica et Cosmochimica Acta* 59:1729–47.

White, A.F., A.E. Blum, T.D. Bullen, D.V. Vivit, M.S. Schulz, and J. Fitzpatrick. 1999b. The effect of temperature on experimental and natural weathering rates of granitoid rocks. *Geochimica et Cosmochimica Acta* 63:3277–91.

White, A.F., and S.L. Brantley. 1995. Chemical weathering rates of silicate minerals: An overview. *Reviews in Mineralogy* 31:1–22.

White A.F., T.D. Bullen, D.V. Vivit, and M.S. Schulz. 1999a. The role of disseminated calcite in the chemical weathering of granitoid rocks. *Geochimica et Cosmochimica Acta* 63:1939–53.

White, A.F., T.D. Bullen, M.S. Schulz, A.E. Blum, T.G. Huntington, and N.E. Peters. 2001. Differential rates of feldspar weathering in granitic regoliths. *Geochimica et Cosmochimica Acta* 65:847–69.

Willett, S.D. 1999. Orogeny and orography: The effects of erosion on the structure of mountain belts. *Journal of Geophysical Research* 104:28957–81.

Willett, S.D., R. Slingerland, and N. Hovius. 2001. Uplift, shortening, and steady state topography in active mountain belts. *American Journal of Science* 301:455–85.

Yanai, R.D., T.G. Siccama, M.A. Arthur, C.A. Federer, and A.J. Friedland. 1999. Accumulation and depletion of base cations in forest floors in the northeastern United States. *Ecology* 80:2774–87.